Multielectron energy structure and physical properties of the ferromagnetic semiconductor CdCr$_2$Se$_4$

V. A. Gavrichkov, M. Sh. Erukhimov, S. G. Ovchinnikov, and I. S. Édel'man

L. V. Kirenskiĭ Institute of Physics, Siberian Division, USSR Academy of Sciences

We propose a multielectron model that takes into account in the zeroth approximation the independent band states and localized ionic states of Cr^{2+}, Cr^{3+}, and Cr^{4+}. The exchange interaction and the hybridization of the band and localized states are perturbations. The quasiparticle spectrum and the density of the single-particle states are found, and the absorption spectrum is calculated. The absorption spectrum of thin CdCr$_2$Se$_4$ films was obtained experimentally up to ~ 3 eV, and its dependence on temperature and doping are investigated. The parameters of the model are determined from a comparison of the experimental and theoretical results. The theory explains also certain electric properties of weakly doped semiconductors.

INTRODUCTION

The electronic structure of the magnetic semiconductors (MS) ACr$_2$X$_4$ (chalcogenide chromium spinels) has been debated for a long time. The existing different models of the energy structure are based on two fundamentally different viewpoints.

On the one side are the band calculations, which have made it possible to determine the dispersion law and the density of states of the conduction band, the valence (mainly s- and p-type) band, and the d-band.[1-3] Since these are essentially single-electron calculations, they do not take due account of the strong intra-atom correlations of the d electrons. Thus, for example, a spin separation of the d-bands is necessary to explain the spin $S = 3/2$ of the Cr^{3+} ion in the X method. Such an approach is apparently correct for the ferromagnetic ground state at $T = 0$ K. In the paramagnetic phase, however, the bands should be spin-degenerate, since the Hamiltonian of the system is isotropic in the absence of an external field. The d-ion spin in the paraphase should therefore be zero, contradicting naturally Hund's rule, the Curie-Weiss law in the paramagnetic phase, and other experimental data. Of course, at the present status of the band theory of magnetism it is possible to take into account strong correlations in the spirit of Hubbard's model, for example in the path-integration scheme,[4] and such calculations were performed for $3d$ metals.[5] No such calculations were made for magnetic semiconductors.

On the other side we have models that take into account strong intra-atom correlations of d electrons even in the first step.[6-11] The first of them are purely empirical in nature and are inconsistent in the sense that energies $E(d^n)$ of multiparticle terms, e.g., of the ions Cr^{3+}, Cr^{2+}, and others, are located on the single-particle electron-energy scale of the conduction bands (hereafter referred to as c-bands). In fact, only atomic resonances with energies $\Omega = E(d^{n+1}) - E(d^n)$ have a single-particle nature and can be set in correspondence with the band-electron energies. Such resonances appear in natural fashion in multielectron solid-state theory when the Hubbard atomic operators are used.

A more consistent model is that of the narrow-band MS (Ref. 9), in which it is assumed that strong intra-atom s-d exchange interaction forms terms d^n with spin S and cd^n with spin $S \pm 1/2$ (depending on the sign of the s-d exchange integral J). These terms are interpreted in Ref. 9 as states of the Cr^{3+} and Cr^{2+} ions. In this approach, the electron jumps between the atoms correspond to motion of the "incorrect" spin $S \pm 1/2$ against the background of the lattice of "correct" spins S. The ensuing band of quasiparticles (spinpolarons in the terminology of Refs. 9 and 12) has a many-particle character and is the consequence of the dispersion of the level introduced above: $\Omega = E(\text{Cr}^{2+}) - E(\text{Cr}^{3+})$. This model has explained qualitatively a number of physical properties of the considered MS. An important feature of the model of Ref. 9 is the d-like character of the quasiparticles of the narrow conduction band; the s and p electrons that form broad c-bands are disregarded. This is possible if the c-bands lie substantially higher than the d-bands. At the same time, band calculations[2] for CdCr$_2$S$_4$ and CdCr$_2$Se$_4$ have shown that s and p orbitals of nonmagnetic ions, as well as d orbitals of chromium, are present near the bottom of the conduction band. In addition, optical[13-15] and magneto-optical[16-18] measurement results, photoconductivity data,[19-22] and also photoemission spectroscopy results[23] point to the presence of a number of singularities in the spectra. These singularities were interpreted as d-resonances due to participation of terms of the ground and excited states of the ions Cr^2, Cr^{3+}, Cr^{4+} (Refs. 24 and 25). These additional resonances, as well as the contributions of the s and p electrons near the bottom of the conduction band, were not taken into account in the model of Ref. 9.

Another variant of a many-electron model of MS was proposed in Ref. 10, in which two terms $^4A_2(\text{Cr}^{3+})$ and $^3T_1(\text{Cr}^{2+})$ were considered besides the single-electron c and b states. Hybridization of the band c states with the atomic d resonance Ω leads to splitting of the conduction band into two hybridized subbands which have, as in Ref. 9, a many-
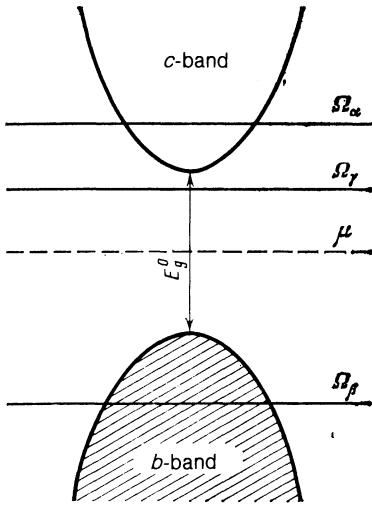
FIG. 1. Energy structure of MS in the absence of c, b–d exchange and c,b–d hybridization.

particle character. The calculation of the absorption spectrum in that reference explained quantitatively the frequency singularities of the absorption edges in $CdCr_2S_4$ and $CdCr_2Se_4$ and their temperature dependences. The theory and experiment, however, were not compared in detail.

We propose in this paper a generalization of the model of Ref. 10, with account taken of the ground states of the ions Cr^{2+}, Cr^{3+} and Cr^{4+}, and also of the first excited state of the Cr^{2+} ion. The need for considering two states of Cr^{2+} is due to the proximity of the energies of the high-spin ($S = 2$) and low-spin ($S = 1$) states of this ion. We obtain the spectrum of the quasiparticles and the density of the single-particle states, and calculate the optical-absorption spectrum at different temperatures. The absorption spectra are obtained experimentally for thin $CdCr_2Se_4$ films up to an energy ~ 3 eV, as functions of temperature and with a donor dopant. A detailed comparison of the calculation results and the experimental data yields all the parameters of the model. The theory explains also certain electric properties of weakly doped p- and n-type $CdCr_2Se_4$ semiconductors.

1. HAMILTONIAN. ELECTRON SPECTRUM

The compound $CdCr_2Se_4$ has a normal spinel structure. The nearest surrounding of the Cd and Cr cations are Se anions, the Cd and Cr cations being respectively in tetrahedral and octahedral positions. The outer shells of the atomic configurations are $5s^2$(Cd), $4s^2 3d^3$(Cr), $4p^4$(Se). When the atoms are joined in the crystal, all the s and p states of the cations and anions become hybridized and form wide bands; an empty conduction c-band and a filled valence b-band. The interaction between the band electrons is weak compared with the widths W_c and W_b of the bands.

The d electrons in chromium are mainly localized and make up the magnetic moment of the crystal. Their intreatomic Coulomb interaction is large compared with the level widths. It is therefore convenient to describe the c and b electrons within the framework of the band approach, and

the d electrons in the language of many-electron atomic configurations. The trivalent chromium ion in $CdCr_2Se_4$ has a $3d^3$ electron configuration. Its three d electrons fill exactly one half of the lower-energy t_{2g} shell, so that the ground state $^4A_2$ of the Cr^{3+} ion is orbitally nondegenerate and corresponds to $S = 3/2$. When the number of electrons in the d shell is changed, the ions Cr^{2+} (d^4) and Cr^{4+} (d^2) are produced. The term energies of the ions Cr^{2+}, Cr^{3+} and Cr^{4+} in $CdCr_2Se_4$ were calculated in Ref. 25, where the Racah coefficients and the crystal-field strength were obtained from a comparison with magneto-optical measurement data.

Figure 1 shows, in accordance with Ref. 25, the energy structure of $CdCr_2Se_4$ in the absence of interaction between the c, b, and d electrons. Besides the conduction and valence band, the figure shows three d-resonances:

$$\Omega_\alpha = E_2 - E_0, \quad \Omega_\beta = E_0 - E_1,$$
$$\Omega_\gamma = E_3 - E_0,$$

where E_0 is the energy of the term $^4A_2$(Cr^{3+}), E_1 the energy of the term $^3T_1$(Cr^{4+}), E_2 and E_3 are the energies of the low-spin and high-spin terms $^3T_1$ and ^5E of the Cr^{2+} ion. The higher-lying terms of the chromium ions will be neglected, since they have little effect on the energy structure in the considered energy interval $\sim \Omega_\alpha - \Omega_\beta$. The spectrum of the noninteracting band and atomic states is described by the Hamiltonian H_0. The total Hamiltonian of the model is

$$H = H_0 + H_1, \tag{1}$$

$$H_0 = H_{0c} + H_{0b} + H_{0d}, \tag{2}$$

$$H_{0c} = \sum_{k\sigma} \xi_c(k) c_{k\sigma}^+ c_{k\sigma}, \quad H_{0b} = \sum_{k\sigma} \xi_b(k) b_{k\sigma}^+ b_{k\sigma},$$

$$H_{0d} = \sum_f \left\{ (E_0 - 3\mu) \sum_{i=1}^{4} X_f^{ii} + (E_2 - 4\mu) \sum_{i=5}^{7} X_f^{ii} \right.$$

$$\left. + (E_1 - 2\mu) \sum_{i=8}^{10} X_f^{ii} + (E_3 - 4\mu) \sum_{i=11}^{15} X_f^{ii} \right\},$$

$$H_1 = \sum_f \left\{ -J_c \sigma_{cf} S_f - J_b \sigma_{bf} S_f + V_c \sum_\sigma (c_{f\sigma}^+ d_{f\sigma} + \text{H.a.}) \right.$$

$$\left. + V_b \sum_\sigma (b_{f\sigma}^+ d_{f\sigma} + \text{H.a.}) \right\}. \tag{3}$$

Here $c_{k\sigma}$ and $b_{k\sigma}$ are the Fermi annihilation operators for electrons with momentum k and spin projection σ in the conduction and valence bands; $\xi_c(k) = \varepsilon_c(k) - \mu$ and $\xi_b(k) = \varepsilon_b(k) - \mu$ are the energies of these electrons, reckoned from the chemical potential μ; $X_f^{pq} = |fp\rangle\langle fq|$ are the Hubbard operators[26] that describe the transition of the chromium ion of the lattice site f from a localized state $|q\rangle$ into a state $|p\rangle$; S_f is the d-ion spin operator; σ_{cf} and σ_{bf} are the spin operators of the c and b electrons; J_c and J_b are the exchange-interaction constants of the atomic and corresponding band electrons;

$$d_{f\sigma} = \sum_{pq} \langle p | d_{f\sigma} | q \rangle X_f^{pq}$$

is the d-electron annihilation operator in the representation of the operator H_0; V_c and V_b are the c–d and b–d electron

hybridization parameters.

The first two terms of (3) describe, just as in the s–d model, exchange interaction of atomic electrons with conduction- and valence-band electrons. The third and fourth terms in (3) correspond to hybridization of the band and atomic state in the sense of Anderson's periodic model. They describe the mixing of the band and atomic states that enter in H_0, since the latter are not eigenstate of the entire crystal. There are many hybridization mechanisms both single-particle (matrix elements $\langle c|H|d\rangle$) and multiparticle (elements of type $\langle cd|H|dd\rangle$). These mechanisms as well as their consequences were considered in detail in Refs. 27–29. Recall that for the band structure the main consequence of hybridization is the smearing of the σ-like peaks in the vicinity of the d-electron states in narrow bands. We do not take into account here the obvious symmetry of the wave functions of the c and b electrons, and do not calculate the matrix elements J_c, J_b and V_c, V_b. They are phenomenological parameters and will be determined by comparison with experiment.

The level E_0 for the $^4A_2$ is fourfold spin-degenerate in the paramagnetic phase, and the indices $i = 1$–4 number the states of the Cr^{3+} ion:

$$|1\rangle=|S=^3/_2;\ S^z=^3/_2\rangle,$$

$$|2\rangle=|^3/_2;\ ^1/_2\rangle,\ |3\rangle|^3/_2;\ -^1/_2\rangle,\ |4\rangle|^3/_2;\ -^3/_2\rangle.$$

For Cr^{4+}, the level $E_1(^3T_1)$ is triply spin-dengenerate:

$$|8\rangle=|d^2;\ S=1;\ S^z=1\rangle,\ |9\rangle d^2;\ 1;\ 0\rangle,\ |10\rangle|d^2;\ 1;\ -1\rangle.$$

For the isospin state ($^3T_1$, level E_2) of the Cr^{3+} ion we have similarly

$$|5\rangle=|d^4;\ 1;\ 1\rangle,\quad |6\rangle=|d^4;\ 1;\ 0\rangle,\quad |7\rangle=|d^4;\ 1;\ -1\rangle,$$

and for the high-spin state (^5E, level E_3),

$$|11\rangle=|2;\ 2\rangle,\ |12\rangle=|2;\ 1\rangle,\ |13\rangle=|2;\ 0\rangle,$$

$$|14\rangle=|2;\ -1\rangle,\ |15\rangle=|2;\ -2\rangle.$$

We shall assume these 15 states to constitute the complete set of atomic states:

$$\sum_{i=1}^{15} X_f^{ii}=1. \tag{4}$$

Any single-site operator Q_f is [26]

$$Q_f=\sum_{pq}\langle p|Q_f|q\rangle X_f^{pq},$$

and in particular, the connection between the spin operators and the Hubbard operators is determined by the formulas

$$S_f^+=3^{1/2}X_f^{1,2}+2X_f^{2,3}+3^{1/2}X_f^{3,4}$$
$$+2^{1/2}(X_f^{5,6}+X_f^{6,7})+2^{1/2}(X_f^{8,9}+X_f^{9,10})$$
$$+2X_f^{11,12}+6^{1/2}(X_f^{12,13}+X_f^{13,14})+2X_f^{14,15},\quad S_f^-=(S_f^+)^+,$$
$$\tag{5}$$

$$S_f^z=^3/_2X_f^{1,1}+^1/_2X_f^{2,2}-^1/_2X_f^{3,3}-^3/_2X_f^{4,4}$$
$$+X_f^{5,5}-X_f^{7,7}+X_f^{8,8}$$
$$-X_f^{10,10}+2X_f^{11,11}+X_f^{12,12}-X_f^{14,14}-2X_f^{15,15}.$$

Equations (5) conserve exactly the spin commutation rela-

tions. The single-particle operator $d_{f\sigma}$ is expressed in similar fashion:

$$d_{f\sigma}=\beta_{f\sigma}+\eta(\sigma)\alpha_{f\sigma}+\gamma_{f\sigma},$$

$$\beta_{f\uparrow}=X_f^{8,1}+(^2/_3)^{1/2}X_f^{9,2}+(^1/_3)^{1/2}X_f^{10,3},$$

$$\beta_{f\downarrow}=X_f^{10,4}+(^2/_3)^{1/2}X_f^{9,3}+(^1/_3)^{1/2}X_f^{8,2},$$

$$\alpha_{f\uparrow}=X_f^{4,7}+(^2/_3)^{1/2}X_f^{3,6}+(^1/_3)^{1/2}X_f^{2,5},$$

$$\alpha_{f\downarrow}=X_f^{1,5}+(^2/_3)^{1/2}X_f^{2,6}+(^1/_3)^{1/2}X_f^{3,7}, \tag{6}$$

$$\gamma_{f\uparrow}=X_f^{1,11}+^1/_2\cdot3^{1/2}X_f^{2,12}+(^1/_2)^{1/2}X_f^{3,13}+^1/_2X_f^{4,14},$$

$$\gamma_{f\downarrow}=X_f^{4,15}+^1/_2\cdot3^{1/2}X_f^{3,14}+(^1/_2)^{1/2}X_f^{2,13}+^1/_2X_f^{1,12}.$$

The operators $d_{f\sigma}$ in the representation (6) are quasi-Fermi operators, since no account was taken of the higher excited states of the chromium ions. The operators $\beta_{f\sigma}$, $\alpha_{f\sigma}$ and $\gamma_{f\sigma}$ are respectively the d-electron annihilation operators in the states $^4A_2$ (transition $^4A_2\to{}^3T_1(Cr^{4+})$), $^3T_1(^3T_1(Cr^{2+})\to{}^4A_2)$, $^5E(^5E(Cr^{2+})\to{}^4A_2)$.

Their Fourier transforms are

$$B_{k\sigma}=N^{-1/2}\sum_f e^{-ikf}B_{f\sigma},\quad B_{f\sigma}=\alpha_{f\sigma},\ \beta_{f\sigma},\ \gamma_{f\sigma}. \tag{7}$$

To determine the electron spectrum, we search for the matrix Green's functions [30]

$$G_{k\sigma}^c(E)=\langle\!\langle\varkappa_{k\sigma}|\varkappa_{k\sigma}^+\rangle\!\rangle_E,\quad G_{k\sigma}^b(E)=\langle\!\langle\lambda_{k\sigma}|\lambda_{k\sigma}^+\rangle\!\rangle_E,$$

where

$$\varkappa_{k\sigma}^+=(c_{k\sigma}^+,\ \alpha_{k\sigma}^+/\sqrt{K_\alpha^\sigma},\ \gamma_{k\sigma}^+/\sqrt{K_\gamma^\sigma}),\quad \lambda_{k\sigma}^+=(b_{k\sigma}^+,\ \beta_{k\sigma}^+/\sqrt{K_\beta^\sigma}). \tag{8}$$

We introduce the notation

$$\xi_\lambda(k,\sigma)=\xi_\lambda(k)-^1/_2J_\lambda\eta(\sigma)\langle S^z\rangle,$$

$$\lambda=c,b,\quad \eta(\sigma)=\begin{cases}+1,&\sigma=\uparrow,\\-1,&\sigma=\downarrow,\end{cases}$$
$$\tag{9}$$

$$\xi_{B\sigma}=\Omega_B-\mu-^1/_2\eta(\sigma)(J_c\langle\sigma_c^z\rangle+J_b\langle\sigma_b^z\rangle),\quad B=\alpha,\ \beta,\ \gamma,$$
$$K_B^\sigma=\langle B_{f\sigma}B_{f\sigma}^++B_{f\sigma}^+B_{f\sigma}\rangle.$$

Using (4) and (6) we obtain

$$K_\alpha^\sigma=^1/_3(^3/_2-\eta(\sigma)\langle S^z\rangle),\quad K_\beta^\sigma=^1/_3(^3/_2+\eta(\sigma)\langle S^z\rangle),$$

$$K_\gamma^\sigma=^1/_4(^5/_2+\eta(\sigma)\langle S^z\rangle). \tag{10}$$

In standard fashion we obtain in the Hartree-Fock approximation

$$G_{k\sigma}^c(E)=(E\hat{I}-\hat{\Omega}_{k\sigma}^c)^{-1},\quad G_{k\sigma}^b(E)=(E\hat{I}-\hat{\Omega}_{k\sigma}^b)^{-1},$$

$$\hat{\Omega}^c=\begin{pmatrix}\xi_c(k,\sigma)&\eta(\sigma)V_c\sqrt{K_\alpha^\sigma}&V_c\sqrt{K_\gamma^\sigma}\\\eta(\sigma)V_c^*\sqrt{K_\alpha^\sigma}&\xi_{\alpha\sigma}&0\\V_c\sqrt{K_\gamma^\sigma}&0&\xi_{\gamma\sigma}\end{pmatrix},$$

$$\hat{\Omega}^b=\begin{pmatrix}\xi_b(k,\sigma)&V_b\sqrt{K_\beta^\sigma}\\V_b\sqrt{K_\beta^\sigma}&\xi_{\beta\sigma}\end{pmatrix}. \tag{11}$$

The poles of the Green's functions $G_{k\sigma}^c(E)$ (11) determine six branches of the conduction electron spectrum: $E^i(k,\sigma)$, $i = 1$–3. The unrenormalized spectrum shown in

Fig. 1 is split into three subbands i as a result of hybridization of the c-states with the atomic states corresponding to the levels Ω_α and Ω_γ. Spin degeneracy takes place in the paramagnetic phase and is lifted in the ferromagnetic region of temperatures as a result of the c–d hybridization itself and of the c–d exchange. The temperature dependence of the spectrum is determined by the values of the magnetization: $\langle S^z \rangle$, $\langle \sigma_c^z \rangle$, and $\langle \sigma_b^z \rangle$, and to find them we must either add to the Hamiltonian (1) a Heisenberg-type term with an effective integral J_{eff} due to various indirect-exchange mechanisms, or else use the experimental dependence of the magnetization on the temperature. For a proper MS we have $\langle \sigma_c^z \rangle = \langle \sigma_b^z \rangle = 0$. Since the dispersion equation is determined by a 3×3 determinant, there is no simple analytic expression for the conduction-electron spectrum, which must be calculated by a numerical method. The (2×2) matrix $\widehat{G}_{k\sigma}^b$ determines the valence-band electron spectrum in the form

$$E^\pm(\mathbf{k}, \sigma) = \tfrac{1}{2}[\xi_b(\mathbf{k}, \sigma) + \xi_{\beta\sigma}] \pm v_{\mathbf{k}\sigma},$$

$$v_{\mathbf{k}\sigma}^2 = \tfrac{1}{4}[\xi_b(\mathbf{k}, \sigma) - \xi_{\beta\sigma}]^2 + K_\beta^\sigma V_b^2. \tag{12}$$

The valence band consists of two hybridized subbands, which are also spin-split in the ferromagnetic phase and are degenerate in the paraphase. The splitting is determined by the magnetization $\langle S^z(T) \rangle$.

2. DENSITY OF STATES

Knowing the Green's functions $G_{k\sigma}^c(E)$ and $G_{k\sigma}^b(E)$, we can find the densities $N_c(E)$ and $N_b(E)$ of the electronic states in the conduction and valence bands:

$$N^\sigma(E) = \frac{1}{N} \sum_{\mathbf{k}i} g_\sigma{}^i(\mathbf{k}) \delta(E - E^i(\mathbf{k}, \sigma)), \tag{13}$$

where the subscript i takes on five values in accordance with the number of $E^i(\mathbf{k}, \sigma)$ bands. Assume that the unperturbed dispersion law for the c and b electrons is of the form

$$\xi_c(\mathbf{k}) = E_g^0/2 + \gamma_{\mathbf{k}}^c, \quad \xi_b(\mathbf{k}) = -E_g^0/2 - \gamma_{\mathbf{k}}^b, \tag{14}$$

where E_g^0 is the width of the unrenormalized gap of the MS (see Fig. 1). Changing in (13) to integration with respect to $\varepsilon = \gamma_{\mathbf{k}}^b$ with a density $N_0(\varepsilon)$ of the unrenormalized valence-band states, we obtain

$$N_b^\sigma(E) = \left\{ \frac{g_\sigma^+(\varepsilon_\sigma) N_0(\varepsilon_\sigma)}{v^2(\varepsilon_\sigma)} + \frac{g_\sigma^-(\varepsilon_\sigma) N_0(\varepsilon_\sigma)}{u^2(\varepsilon_\sigma)} \right\} \int d\varepsilon \, \delta(\varepsilon - \varepsilon_\sigma), \tag{15}$$

where we have for the function $g_\sigma^i(\varepsilon_\sigma)$ of the degeneracy degree of the level of energy E

$$g_\sigma^+(\varepsilon_\sigma) = v^2(\varepsilon_\sigma) + K_\beta^\sigma u^2(\varepsilon_\sigma), \quad g_\sigma^-(\varepsilon_\sigma) = u^2(\varepsilon_\sigma) + K_\beta^\sigma v^2(\varepsilon_\sigma),$$

$$u^2(\varepsilon_\sigma) = \frac{1}{2}\left[1 - \frac{\xi_b(\varepsilon_\sigma, \sigma) - \xi_{\beta\sigma}}{v_\sigma(\varepsilon_\sigma)}\right],$$

$$v^2(\varepsilon_\sigma) = \frac{1}{2}\left[1 + \frac{\xi_b(\varepsilon_\sigma, \sigma) - \xi_{\beta\sigma}}{v_\sigma(\varepsilon_\sigma)}\right]$$

$$\varepsilon_\sigma = -\tfrac{1}{2}E_g^0 - \tfrac{1}{2}J_b\eta(\sigma)\langle S^z \rangle - E + K_\beta^\sigma V_b^2/(E - \xi_{\beta\sigma}).$$

Let us discuss qualitatively the difference between the single-particle density of states in the one- and many-elec-

tron approaches. We know that in the band theory the influence of the magnetic order reduces to a separation of the bands. In our theory, the variation of the density of state (15) with temperature is shown in the lower part of Fig. 2. It can be seen that the amplitudes of the x-peaks vary without changing the d-state energy. The level shifts Ω_B are made possible by the Heisenberg exchange, but they are of the order of the Curie temperature T_C and are much smaller than the exchange integrals J_c and J_b which describe the shifts of the c and b bands.

The zero density of d-states with down-spin at $T = 0$ K is due to the fact that the factor $K_\beta^{\downarrow}$ $(T = 0 \text{ K}) = 0$. This means physically that in a fully ordered phase transitions between the terms $^4A_2(\text{Cr}^{3+}$ with $S^z = 3/2$ and $^3T_1$ (Cr^{4+} with $S^z = 1$) are possible only for d_1 electrons with up-spin and are impossible for down-spins. We note that the existence of localized peaks that are immobile when the temperature changes is observed not only in the considered MS, but also in a number of rare-earth metals, such as gadolinium.[31] We can similarly calculate the density of states for the conduction electrons, but shall not present the analytic expressions here, since they were obtained only by numerical means. If hybridization with only one term of Cr^{2+} were to be considered, the spectrum could be calculated analytically and an equation of the form (15) would be obtained for the density of states.

The present model contains a large number of unknown parameters: E_g^0, Ω_α, Ω_β, Ω_γ, J_b, J_c, V_b, V_c, as well as the widths W_c and W_b [Eq. (14)] of the unrenormalized bands. These parameters can be calculated in principle, for example, in the Hartree-Fock approximation. Whereas, however, the eigenvalues (energies) are calculated quite satisfactorily in modern band theory, the interaction matrix elements are much harder to calculate. The computations on the whole are very laborious and their reliability is uncertain. We used therefore a different method, that of obtaining the parameters from experiment. It might seem at first glance that any experimental curve can be described by ten parameters, so that the problem of determining the parameters from experiment yields many different parameter sets. Actually, we can describe one experimental curve at a given temperature by several methods, but then, by varying the temperature in a wide range without changing the parameters, we compare the calculation with experiment at different temperatures. Most parameter sets are excluded thereby and only a few remain. It was found in addition that the parameters can be grouped into essential and inessential, in the sense that small changes of the essential ones influence strongly the electron spectrum and the density of states. In our case the essential parameters are E_g^0, Ω_γ, Ω_β, J_b, J_c, V_c. The remaining parameters are inessential in the sense that a small change of such a parameter has little effect on the calculation results. The values obtained for the essential parameters are therefore more accurate (~ 0.1 eV) and those of the inessential less accurate.

Figure 2 shows plots of the density of states of CdCr_2Se_4, obtained by us at various temperatures after determining the model parameters from optical and magneto-
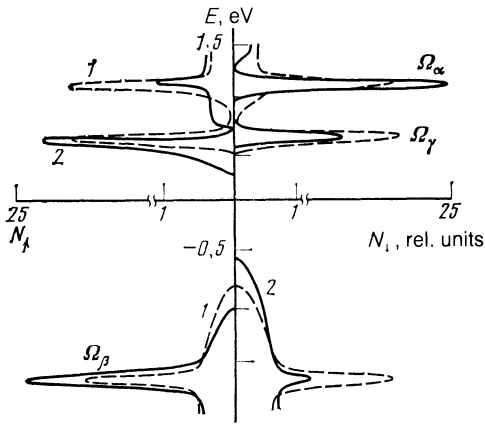
FIG. 2. Density of states of $CdCr_2Se_4$, calculated from Eq. (13). Curves 1 and 2 correspond to temperatures 300 and 4 K.

optical data. For clarity, the heights of all peaks corresponding to the d states have been decreased by a factor of ten. The energy origin, as in Fig. 1 is the middle of the unrenormalized gap E_g^0. The peak at -1.7 eV corresponds to the resonance Ω_β, and the peaks at 0.6 and 1.1 eV correspond respectively to resonances Ω_γ and Ω_α. The resonance Ω_β lies $\tilde{\Omega}_\beta = -E_g^0/2 - \Omega_\beta \approx 0.9$ eV lower than the top of the valence band in the paraphase, at a height of the order of $\tilde{\Omega}_\beta = 1.45 \pm 0.3$ eV obtained from experiments on x-ray photoemission, and of the order of $\tilde{\Omega}_\beta = 0.4$ eV obtained from band calculations[2] for spin-up d states (d_ε states in the notation of Ref. 2). Recognizing that the theory parameters themselves were obtained by comparison with other experiments with nonzero errors, we estimate the error in the determination of the parameters E_g^0 and Ω_β at approximately 0.1 eV. The agreement between our calculation and the data of Ref. 23 can then be regarded as satisfactory. The contribution, contained in the band picture,[2] of d_γ states with spin down (1 eV lower than the valence-band top) correspond in our model to a resonance with participation of an excited state of Cr^{4+} and lies even lower in the valence band. As already mentioned, we disregard such states here.

The following features of the density of states of the conduction electrons are noteworthy. First, c–d hybridization causes a narrow band $\Omega_\gamma(E)$ to be split off. The existence of such a band was proposed in the narrow-band model[9]; in our model this band contains hybridized c–d states, and the contribution of the c states on the bottom of the band increases with decreasing temperature.

Second, the temperature dependence of the width of the narrow band $\Omega_\gamma(E)$ is due both to c–d exchange and to c–d hybridization on account of the factor $K_\gamma^\sigma(T)$ in (9). Since $K_\gamma^\sigma \neq 0$, the density of the d states of the $\Omega_\gamma^\sigma(E)$ subbands does not vanish (in contrast to the $\Omega_\beta^\sigma(E)$ band) at any temperature. Physically this means that two Ω_γ resonances are possible for the high-spin Cr^{2+}

$$|^3/_2;\ ^3/_2\rangle + d_\uparrow \leftrightarrow |2;\ 2\rangle, \quad |^3/_2;\ ^3/_2\rangle + d_\downarrow \leftrightarrow |2;\ 1\rangle.$$

The temperature dependence of the $\Omega_\alpha(E)$ band is similar to that considered above for the $\Omega_\beta(E)$ band. At $T = 0$, only

the density of states differs from zero, since only one resonance is possible for the low-spin Cr^{2+}:

$$|^3/_2;\ ^3/_2\rangle + d_\downarrow \leftrightarrow |1;\ 1\rangle.$$

In the band calculations[2] there is a narrow band $d_\gamma^\uparrow(E)$ of width ~ 0.5 eV near the bottom of the conduction band, corresponding to our $\Omega_\gamma^\uparrow(E)$ band. At the same time, for down spin the density of states of Ref. 2 differs greatly from ours: the bands $d_\gamma^\downarrow$ and $d_\varepsilon^\downarrow$ changed places, and the separation was $d_\gamma^\downarrow - d_\gamma^\uparrow \approx 3$ eV, whereas in our case the resonances Ω_γ and Ω_α can be separated only by $\sim T_C$. As we have noted above, these large spin splittings of the d bands are the shortcoming of the band calculations.

3. ABSORPTION SPECTRA: THEORY AND EXPERIMENT

The interaction of light with matter is described in the dipole approximation by the Hamiltonian

$$H_{int} = -\frac{E}{\omega} e^{-i\omega t} \sum_{k\sigma ij} d_{ij}\omega_{ij}^0(\mathbf{k})\ (i_{k\sigma}^+ j_{k\sigma} - j_{k\sigma}^+ i_{k\sigma}), \quad i = c, \alpha, \gamma,$$

$$j = b, \beta, \quad \omega_{ij}^0(\mathbf{k}) = \xi_i(\mathbf{k}) - \xi_j(\mathbf{k}). \tag{16}$$

The light-absorption coefficient is calculated in standard fashion with the aid of two-time Green's functions.[32] For each spin projection, the absorption can be due to transitions from two valence bands into all three bands of the conduction electrons. Therefore the absorption coefficient is of the form

$$K(\omega) = \sum_{i\lambda\sigma} K_{\lambda i}(\omega, \sigma), \quad i = b, \beta, \quad \lambda = \alpha, \gamma, c,$$

$$K_{\lambda i}(\omega, \sigma) = \frac{\hbar m^*}{2\pi} \int dk\, F_{\lambda i}(\mathbf{k})\, \delta(\hbar\omega - \hbar\omega_{\lambda i}(\mathbf{k}, \sigma)), \tag{17}$$

$$\omega_{\lambda i}(\mathbf{k}, \sigma) = \hbar^{-1}[E^\lambda(\mathbf{k}, \sigma) - E^i(\mathbf{k}, \sigma)],$$

where $F_{\lambda i}(\mathbf{k})$ is the oscillator strength of the quantum transition between the bands, and is determined from the known band structure by a numerical method; $m^* = m_e m_h/(m_e + m_h)$.

The calculation of the absorption spectrum at different values of the model parameters and temperatures was compared with experiments on light absorption in thin $CdCr_2Se_4$ films. The absence of skin effect in the films made it possible to advance to frequencies corresponding to ~ 3 eV and observe new singularities of the spectrum besides the known singularities at the absorption edge. One can distinguish on the experimental curve of Fig. 3 three singularities: A—at a frequency 1.1–1.4 eV, which splits at $T < T_C$ on the optical absorption edge E_{g1} and a higher-energy singularity E_{g2} (see Fig. 6). Both singularities, E_{g1} and E_{g2}, undergo a red shift with decreasing temperature. The second singularity (B) at ~ 1.7 eV experiences a deep shift in the magnetically-ordered phase, while the third, C, has at 2.2 eV a peak that varies in amplitude but whose frequency is practically independent of temperature.

The crucial factor in the comparison of the calculations with experiment is the tie-in of the B-peak to the transition between the subbands $\Omega_\beta(E)$ and $\Omega_\gamma(E)$, which specifies the difference $\Omega_\gamma - \Omega_\beta$. The appearance of the B peak can in
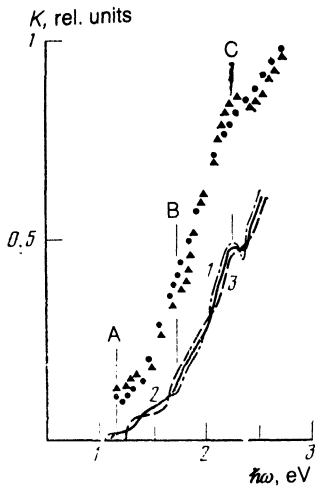
FIG. 3. Absorption spectrum in $CdCr_2Se_4$. Curves (theory): 1—4 K, 2— 78 K, 3—300 K; points (experiment): ▲—78 K, ●—300 K.

FIG. 4. Effect of doping on the amplitude of the B-peak at $T = 35$ K: 1— $CdCr_2Se_4$, 2—$CdCr_2Se_4$ (0.5% In).

principle be attributed to the "parallelism" of the ξ_c (k) and ξ_b (k) dispersion laws on some quasimomentum interval of the Brillouin zone. Such a band mechanism in an MS should lead, however, to a strong temperature dependence of the B-peak frequency, something not observed in experiment. Another important factor is the location of the Ω_γ level relative to the bottom of the c-band. If this level were located deep in the c-band, doping with n-type impurities would not influence the amplitude of the B peak. Figure 4 shows the data obtained by us, for $CdCr_2Se_4$ films, on how doping with indium affects the absorption spectrum in the vicinity of the B-peak. The strong decrease of the amplitude indicates that the Ω_γ level lies near the bottom of the c-band. It was shown in Ref. 10 that, depending on the signs of J_c and J_b, four different density-of-states schemes are possible. Analysis of all four cases has shown that the general form of the absorption curve and its temperature dependence can be satisfactorily explained only for $J_c > 0$ and $J_b > 0$. By variation, we obtained the following parameter values (in eV):

$$E_g^0 = 1.6, \quad W_c = 4, \quad W_b = 3, \quad \Omega_\alpha = 1.1, \quad \Omega_\beta = -1.65,$$

$$\Omega_\gamma = 0.6, \quad J_b = 0.35, \quad J_c = 0.6, \quad V_c = 0.2, \quad V_b = 0.$$

Figure 3 shows also the calculated absorption spectrum for different temperatures and for the parameters indicated above. We used the following values of the dipole matrix elements:

$$d_{bc} = 1, \quad d_{b\gamma} = 0.25, \quad d_{b\alpha} = 0, \quad d_{\beta c} = 0.08, \quad d_{\beta\gamma} = d_{\beta\alpha} = 0.$$

The aforementioned experimental singularities of the spectrum result from the following optical transitions: the absorption edge E_{g1} at $T > T_C$— from the top of the valence band (b state) to hybridized c and d states of the $\Omega_\gamma(E)$ band with matrix elements d_{bc} and $d_{b\gamma}$, while at $T < T_C$— mainly into d states of the $\Omega_\gamma(E)$ band with matrix element $d_{b\gamma}$; the E_{g2} singularity at $T < T_C$— from the top of the valence band into the c states of the $\Omega_\gamma(E)$ band with matrix element d_{bc}; the B singularity—from the top of the valence band to the c states of the $\Omega_\alpha(E)$ band; and the C peak—
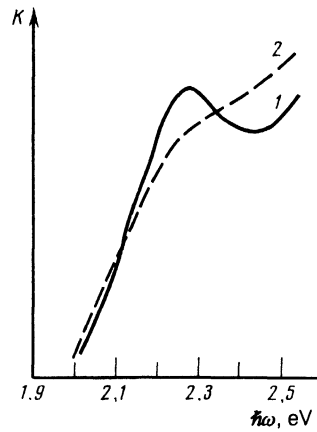
from the d states of the $\Omega_\beta(E)$ band to the c states of the $\Omega_\gamma(E)$ band with matrix element $d_{\beta c}$. Whereas the absorption edge E_{g1} is formed by transitions from the top of the valence band with spin down into the subband, spin-up transitions $b^{'} \rightarrow \Omega_\gamma^{'}$ form the singularity E_{g2} observed in experiment.[13] It is interesting that the optical gap (the transparency region) exceeds in this case the temperature gap by approximately 0.3 eV ($T = 0$).

Figure 5 shows the calculated temperature dependences of the absorption edge E_{g1} and of the singularity E_{g2}, which agree well with the data of Ref. 33 for E_{g1} (T) and of Ref. 13 for E_{g2} (T). The red shift of the E_{g1} edge is due mainly to motion of the top of the valence band with down spin. The red shift of E_{g2} is of more complicated nature, since the top of the valence band with up spin moves down (in energy) together with the bottom of the $\Omega_\gamma^{'}$ subband, but the rates of these shifts have different functional dependences on the temperature. We used in the calculations an elliptic density of states for the unrenormalized c- and b-bands:
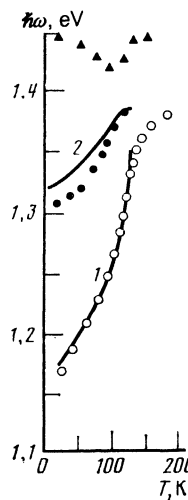
FIG. 5. Temperature dependences of the optical-absorption edge E_{g1} (1,O), of the E_{g2} singularity (2,●), and of the magnetic part of the activation energy (▲). Curves—theory (1—$\sigma = \downarrow$; 2—$\sigma = \uparrow$); points— experiment: O—Ref. 33, ●—Ref. 13.

E, eV
0.06
0
K, rel. un.
a
k
1
0.5
0
1,1   1,2   1,3 $\hbar\omega$, eV

b

E_{g1} E_{g2}

2   3
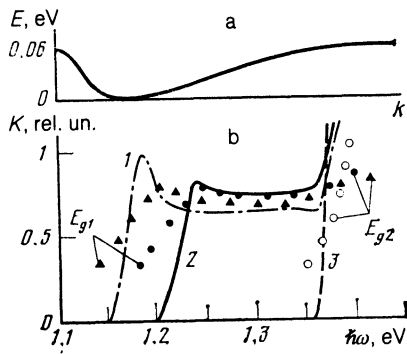
FIG. 6. Schematic dispersion law for the unrenormalized level Ω_γ (a) and the corresponding frequency dependence of the optical-absorption edge (b): 1, 2, 3—theory, points—experiment[14] at temperatures 4.2 (▲), 78 (●).

$$N_0'(\varepsilon) = (2/\pi W_i)[1-(2\varepsilon/W_i)^2]^{1/2},$$
$$i=c, b. \qquad (18)$$

This density of states describes correctly the singularities on the band edges, but does not contain Van Hove singularities in the interior of the band. One might expect the latter to produce their own peaks in the absorption spectrum in band–band transitions. However, a calculation at another density of states, that has singularities both on the edge and in the interior of the band (see Fig. 13 of Ref. 34) did not lead to significant changes in the absorption spectrum. The reason is that for all the discussed characteristic points of the spectrum only the B singularity is connected with band–band transitions, namely from the top of the b-band to the bottom of the c-band. In this case only the band-edge singularities accounted for in (18) are of importance.

Nonetheless, the calculated spectrum of Fig. 3 has no peak at the very edge E_{g1} of the optical absorption. In our opinion, this can be due either to the presence of a heavy-hole subband in the valence band, or to the fact that the edge is formed by transitions predominantly into the d states of the $\Omega_\gamma(E)$ band. The form of the edge can therefore be very sensitive to weak dispersion of the unrenormalized Ω_γ level, a dispersion due not only to hybridization but also to d–d hops between atoms. Figure 6 shows by way of example the schematic dispersion law of narrow $\Omega_\gamma'(\mathbf{k})$ subband (width 0.06 eV, $V_c = 0$) and the corresponding form of the absorption edge.

The band structure of $CdCr_2Se_4$ and its connection with the optical properties was discussed in the three-band model[35] within the framework of the one-electron strong-coupling method. A number of qualitative results of our model agree with those of Ref. 35: narrow d-bands located below the bottom of a wide conduction band and in the interior of the valence band; the negative sign of the effective mass of the d band in the vicinity of the point Γ. At the same time, some details do not agree, such as the nature of the red shift. The parameter of the one-particle one-site s–d hybridization $\langle s|V_{cryst}|d\rangle$ in Ref. 35 is zero. Our phenomenological parameter V_c is determined by all the hybridization mechanisms and need not coincide with the matrix element $\langle s|V_{cryst}|d\rangle$. Two specific mechanisms were proposed in

Ref. 35 for the appearance of nonzero c–d hybridization, viz., allowance for the trigonal component of the crystal field and the contribution of the p states to the wave functions of the c electrons.

4. DISCUSSION OF ELECTRIC PROPERTIES

The parameters J_c and J_b can be determined not only from optical measurements, but also by comparison with the magnetic part of the activation energy $\Delta E_a(T)$ of doped n- and p-type $CdCr_2Se_4$. For the p-type semiconductor, $\Delta E_a(T)$ was determined in Ref. 36 under the assumption that the acceptor level ε_a does not move when the temperature is changed. We denote the energy of the top of the valence band with down spin at a given temperature by $\varepsilon_b(T)$; the magnetic part is then

$$\Delta E_a(T) = \varepsilon_b(T) - \varepsilon_b(300 \text{ K}).$$

Obviously, in our energy-structure variant the sum

$$\Delta = E_{g1}(T) + \Delta E_a(T) = E_{g1}(300 \text{ K}) \qquad (19)$$

does not depend on temperature. In Fig. 5 above, the triangles mark the values of $\Delta(T)$, which were calculated from the data of Ref. 33 for $E_{g1}(T)$ and of Ref. 36 for $\Delta E_a(T)$. It turned out that $\Delta = 1.42 \pm 0.015$ eV for all T. The constancy of Δ is an independent confirmation of the fact that the shift of the absorption edge is due to the shift of the top of the valence band. The parameter $|J_b|$ is determined from the magnetic part of the activation energy and from the known valence-band spectrum (17). This yields $|J_b| = 0.36$ eV, in good agreement with the optically obtained value cited above. We can similarly use the data for n-doping. Figure 7 shows the calculated energies $\varepsilon_c^\uparrow(T)$, $\varepsilon_c^\downarrow(T)$ of the bottom of the conduction band and the measured[36] magnetic part of the $Cd_{1-x}In_xCr_2Se_4$ activation energy. Assuming again that the donor level ε_d does not shift with change of temperature, we get

$$\Delta E_a(T) = \varepsilon_c^\uparrow(300 \text{ K}) - \varepsilon_c^\uparrow(T).$$

E, eV
0,6
0,5
0,4
0,3
0   100   200
T, K

1
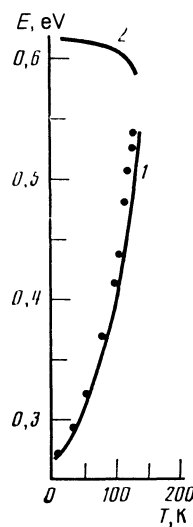
FIG. 7. Shift of the bottom of the conduction band ε_c^σ. Curves 1 ($\sigma = \uparrow$) and 2 ($\sigma = \downarrow$) are theoretical, and the points experimental.[36]

The exchange integral $|J_c| = 0.63$ eV obtained from the activation energy agrees well with the value $J_c = 0.6$ obtained from optical measurements.

We emphasize that the temperature dependence of the bottom of the $\Omega_\gamma (E)$ band is connected with the hybridized c states. Since the contribution of the c states is largest at $T = 0$ K and is decreased by heating, it follows from our model that the mobility of the carriers in n-type semiconductors should decrease in the magnetically ordered phase with increasing T.

CONCLUSION

The proposed multielectron model differs qualitatively from the one-electron variants of the energy structure[1-3] and contains, as particular cases, elements of similar many electron models.[9,10] The agreement between the parameters obtained from the optical properties and from the conduction-activation energy raises hopes that the model can describe also other physical properties determined by the singularities of the energy spectrum. Our model can be quite readily extended to other magnetic semiconductors, such as chalcogenide chromium spinels. Thus, the principal changes of the model for $CdCr_2Se_4$ consist apparently of inversion of the high- and low-spin terms of Cr^{2+} and also of an increase of the band gap E_g^0

The authors thank E. V. Kuz'min for a discussion of the results.

[1]T. Kambura, T. Oguchi, and K. I. Gondaira, J. Phys. C 13, 1493 (1980).

[2]T. Oguchi, T. Kambara, and K. I. Gondaira, Phys. Rev. B 22, 872 (1980).

[3]J. Barvik, Czech. J. Phys. B 33, 331 (1983).

[4]T. Moriya, J. Magn. and Magn. Mater. 14, 1 (1979).

[5]J. Hubbard, Electron Correlation and Magnetism in a Narrow-Band System, N.Y. 1981, p. 29.

[6]J. B. Goodenough, J. Phys. Chem. Sol. 30, 261 (1969).

[7]C. Haas, IMB J. Res. Dev. 14, 282 (1970).

[8]S. Methfessel and D. S. Mattis, Magnetic Semiconductors, in: Handb. Physik Vol. 18, part 1, Springer, 1968, pp. 380–562.

[9]E. L. Nagaev, Physics of Magnetic Semiconductors [in Russian], Nauka, 1979, p. 127.

[10]M. Sh. Erukhimov and S. G. Ovchinnikov, Fiz. Tverd. Tela (Lenin-grad) 21, 351 (1979) [Sov. Phys. Solid State 21, 209 (1979)].

[11]K. M. Golant and V. T. Moshnyaga, Preprint No. 276, FIAN SSSR, 1983.

[12]E. L. Nagaev, Zh. Eksp. Teor. Phys. 56, 1013 (1969) [Sov. Phys. JETP 29, 545 (1969)].

[13]S. Sakai, T. Sugano, and Y. Okabe, Japan J. Appl. Phys. 15, 2023 (1976).

[14]G. Harbeke and H. W. Lehman, Sol. St. Commun. 8, 1281 (1970).

[15]I. S. Edelman, G. Distmuradov, and V. P. Kononov, Phys. Stat. Sol. (b) 117, 351 (1983).

[16]L. L. Golik, Z. E. Kun'kova, T. G. Aminov, and V. T. Kalinnikov, Fiz. Tverd. Tela (Leningrad) 22, 877 (1980) [Sov. Phys. Solid State 22, 512 (1980)].

[17]P. F. Bongers, C. Haas, A. M. Y. G. van Run, and G. J. Zanmarchi, Appl. Phys. 40, 958 (1969).

[18]I. S. Édel'man, V. P. Kononov, G. G. Vasil'ev, et al., Fiz. Tverd. Tela (Leningrad) 20, 3690 (1978) [Sov. Phys. Solid State 20, 2132 (1978)].

[19]T. G. Aminov, V. G. Veselago, G. I. Vinogradova, et al., ibid., 18, 1673 (1974) [18, 971 (1974)].

[20]S. G. Stoyanov, M. N. Iliev, and S. P. Stoyanova, Sol. St. Commun. 18, 1389 (1976).

[21]A. Amith and S. B. Berger, J. Appl. Phys. 42, 1472 (1971).

[22]V. T. Moshnyaga, K. M. Golant, and V. G. Veselago, Zh. Tekh. Fiz. 53, 1473 (1983) [sic].

[23]W. S. Miniscalo, B. C. McCollum, N. G. Stoffel, and G. Margaritondo, Phys. Rev. B 25, 2947 (1982).

[24]S. G. Ovchinnikov, I. S. Édel'man, and G. Dustmuradov, Fiz. Tverd. Tela (Leningrad) 21, 2927 (1979) [Sov. Phys. Solid State 21, 1687 (1979)].

[25]M. Sh. Erukhimov and I. S. Édel'man, Preprint No. 147F, Phys. Inst. Sib. Div. USSR Acad. Sci., 1980.

[26]J. C. Hubbard, Proc. Roy. Soc. A281, 401 (1964).

[27]E. V. Kuz'min, G. A. Petrakovskiĭ, and E. A. Zavadskiĭ, Physics of Magnetically Ordered Substances [in Russian], Nauka, Novosibirsk, 1976, p. 389.

[28]K. A. Kikoin, Zh. Eksp. Teor. Fiz. 85, 1000 (1983) [Sov. Phys. JETP 58, 582 (1983)].

[29]D. I. Khomskiĭ, Usp. Fiz. Nauk 129, 443 (1979) [Sov. Phys. Usp. 22, 879 (1979)].

[30]S. V. Tyablikov, Methods of Quantum Theory of Magnetism [in Russian], Nauka, 1975, p. 528.

[31]A. B. Beznosov, V. P. Gnezdilov, and V. V. Eremenko, Pis'ma Zh. Eksp. Teor. Fiz. 38, 486 (1983) [JETP Lett. 38, 587 (1983)].

[32]A. S. Davydov, Quantum Mechanics [in Russian], Nauka, 1973, p. 462.

[33]G. Harbeke and H. Pinch, Phys. Rev. Lett. 17, 2090 (1966).

[34]I. M. Lifshitz, M. Ya. Azbel', and M. I. Kaganov, Electron Theory of Metals, Consultants Bureau, 1973.

[35]V. G. Vesselago and V. V. Tugushev, Preprint No. 227, Inst. Gen. Phys. USSR Acad. Sci., 1984.

[36]V. K. Chernov and V. N. Berzhanskiĭ, Fiz. Tverd. Tela (Leningrad) 24, 1895 (1982) [Sov. Phys. Solid State 24, 1895 (1982)].

Translated by J. G. Adashko